Nifuroxazide Ameliorates Pulmonary Fibrosis By Blocking Myofibroblast Genesis And Stat3 Activation: A Drug Repurposing Study

Cailing Gan
Sichuan University
Qianyu Zhang
Sichuan University
Hongyao Liu
Sichuan University
Guan Wang
Sichuan University
Liqun Wang
Sichuan University
Yali Li
Sichuan University
Zui Tan
Sichuan University
Wenya Yin
Sichuan University
Yuqin Yao
Sichuan University
Yongmei Xie
Sichuan University
Liang Ouyang
Sichuan University
Luoting Yu
Sichuan University
Tinghong Ye (yeth1309@scu.edu.cn)
Sichuan University https://orcid.org/0000-0002-3296-6753

Research

Keywords: Nifuroxazide, Idiopathic pulmonary fibrosis, TGF-β1, Stat3, EMT

Posted Date: June 15th, 2021

DOI: https://doi.org/10.21203/rs.3.rs-557091/v1

Abstract

Background: Idiopathic pulmonary fibrosis (IPF) is a lung disease with complex pathogenesis, high mortality. The development of new drugs is time-consuming and laborious, and the research on new use of old drugs can save time and clinical costs and even avoid serious side effects. Nifuroxazide (NIF) was originally used to treat diarrhoea, but in recent years it has been found to have other pharmacological effects such as anti-tumor and inhibiting inflammatory diseases related to diabetic nephropathy. However, there are no reports about its role in pulmonary fibrosis.

Methods: The therapeutic effect of NIF on bleomycin (BLM)-induced pulmonary fibrosis *in vivo* was measured by ELISA, hydroxyproline content, H&E and Masson staining, IHC and Western blot. The content of immune cells in lung tissue was analyzed by flow cytometry. NIF cytotoxicity were evaluated in NIH/3T3, Human pulmonary fibroblasts (HPF), A549 and Rat primary lung fibroblasts (RPLF) using MTT assay. Finally, a cell model induced by transforming growth factor-β1 (TGF-β1) stimulation and different *in vitro* experiments (Immunofluorescence, Western blot, Wound migration assay) were conducted to determine the effect of NIF on the activation of fibroblasts and the epithelial-mesenchymal transition (EMT) and migration of epithelial cells.

Results: *In vivo*, intraperitoneal injection of NIF relieved and reversed pulmonary fibrosis caused by BLM bronchial instillation. In addition, nifuroxazide inhibited the expression of a variety of cellular inflammatory factors and immune cells. Furthermore, nifuroxazide suppressed the activation of fibroblasts and the EMT of epithelial cells induced by TGF-β1. Most importantly, we used an analytical docking experiment and thermal shift assay to further verify that nifuroxazide worked in conjunction with Stat3. Moreover, nifuroxazide decreased the expression of p-Stat3 *in vitro* and *in vivo*.

Conclusion: These results suggest that NIF inhibits and reverses pulmonary fibrosis and support NIF as a viable treatment option that may bring benefits to patients with IPF.

Background

Pulmonary fibrosis is a type of chronic, progressive interstitial lung disease, of which idiopathic pulmonary fibrosis (IPF) is the most severe[1]. IPF usually occurs in adults, causing dyspnea and dry cough, and has a median survival of 2–3 years[2, 3]. Pulmonary fibrosis is caused by a variety of factors, such as ageing, genetic factors, environmental factors and various exogenous factors, which lead to the abnormal activation of fibroblasts, the proliferation and persistence of myofibroblasts, and the excessive deposition of collagen and other extracellular matrix (ECM) components, thus destroying lung structure and rapidly reducing lung function[4, 5]. For the treatment of pulmonary fibrosis, there is no widely used programme, although there are two drugs on the market, namely, nintedanib and pirfenidone[6]. However, nintedanib cannot significantly improve the rate of FVC decline in patients with non-advanced pulmonary fibrosis, and the incidence of adverse reactions is 97.2%[7]. Pirfenidone also causes some

gastrointestinal effects, nausea and other adverse reactions[8]. So far, reversing pulmonary fibrosis remains a challenge. Therefore, potential drugs are urgently needed to treat pulmonary fibrosis.

The process of pulmonary fibrosis is regulated by various inflammations and chemokines, and also involves multiple signaling pathways. Transformation growth factor-β1 (TGF-β1) is one of the most effective inducing factors in these molecules[9], and signal transduction and transcription activator 3 (Stat3) signaling pathways are also involved. Stat3 is a transcription factor that regulates many cellular functions, including proliferation, migration, survival and differentiation[10]. In IPF lungs, there are a large number of Stat3-immunopositive cells, which correspond to fibrotic areas[11]. In addition, Stat3 is also a key molecule regulating the phenotype of fibroblasts. According to reports, fibroblasts from keloid lesions show constitutive activation of the Stat3 signalling pathway and that inhibition of this pathway reverses the fibrogenic activity of cells[12]. These evidences indicate that Stat3 is a potential therapeutic target for pulmonary fibrosis.

Given that the discovery and development of new drugs is a very long and extremely costly and time-consuming process, the re-use of “old” drugs to treat common and rare diseases is becoming increasingly attractive because it uses low-risk compounds that may save development costs and shorten time[13]. As an inhibitor of Stat3, nifuroxazide (NIF) was originally used to treat diarrhoea, but in recent years, it has been found to have effects against breast cancer, primary myeloma, hepatocarcinoma and other cancers and promote the immune response against tumours[14–16]. In addition, NIF significantly reduces renal macrophage infiltration and fibrosis in diabetic kidney tissue[17]. However, the role of NIF in IPF has not been reported.

In this study, we found that NIF could ameliorate and reverse bleomycin (BLM)-induced pulmonary fibrosis and that its mechanism may be through regulating Stat3 and inhibiting the EMT and migration of A549 epithelial cells and the activation of fibroblasts to inhibit pulmonary fibrosis. These results suggest that NIF is a potential drug for the treatment of pulmonary fibrosis.

Methods

Reagents and antibodies

NIF was purchased from Xiyashiji Chemical Co., Ltd. (Chengdu, Sichuan, China). The purity (98%) was measured by HPLC analysis. NIF was prepared initially as a 10 mM stock solution in dimethyl sulfoxide (DMSO) and stored at -20°C for *in vitro* assays. For *in vivo* studies, NIF was prepared in a 5:35:60 ratio of DMSO: polyethylene glycol 400: normal saline and administered at a dose of 0.1 mL/10 g body weight. PEG 400 was purchased from Sigma (St. Louis, MO, USA). Thiazolyl blue tetrazolium bromide (MTT) and dimethyl sulfoxide (DMSO) were purchased from Sigma (St Louis, MO). Recombinant human TGF-β1 was purchased from Novoprotein (Shanghai, China). BLM sulfate was purchased from Chengdu Synguider Technology Co., Ltd. (Chengdu, China). Collagenase Type IV was purchased from Gibco (Grand Island, NY, USA). The primary antibodies used in this study were anti-β-actin (Abcam, Cambridge, MA, USA), anti-GAPDH (ZSGB-BIO, Beijing, China), anti-α-SMA actin, anti-Collagen-I, anti-E-Cadherin, anti-

Vimentin (Abcam, Cambridge, MA, USA), and Stat3/phospho-Stat3 (Cell Signalling Technology Company, MA, USA). PE-CD11b-, FITC-Gr-1, PE-F4/80, FITC-CD11b, PE-CD4, APC-CD69, and FITC-CD8-conjugated antibodies were obtained from BD Biosciences (San Diego, CA, USA).

Cell culture

A549 and NIH/3T3 were purchased from American Type Culture Collection (Rockville, MD, USA). HPF (Human pulmonary fibroblast) was purchased from Science Cell (San Diego, CA, USA). All cells were cultured in high-glucose DMEM containing 10% or 20% heat-inactivated foetal bovine serum (FBS; HyClone, Logan, UT, USA) and 1% penicillin and streptomycin (MP Biomedical LLC) in 5% CO_2 at 37°C.

Molecular docking studies

The three-dimensional X-ray crystal structure of Stat3 (PDB ID: 6NJS) was downloaded from the Protein Data Bank. Both the compound and protein were processed using the CHAR Mm force field[18]. Molecular docking was performed using the CDOCKER module in Accelrys Discovery Studio (version 3.5; Accelrys, San Diego, CA, USA). The molecular docking parameters were according to the standard values set by the software. After the docking study was completed, the platform was used to collect the docking score and analyse the docking modes.

MTT assay

The viability of NIF-treated cells was assessed by the MTT assay. Cells in the logarithmic growth phase were inoculated into a 96-well plate at a density of 1000–8000/well and administered NIF (0–20 μM) 24 h later. After 24, 48, or 72 h, 20 μL of 5 mg/mL MTT was added. After 2–4 h at 37℃, the solvent in all wells was aspirated and dissolved in 150 μL of DMSO, and the absorbance was measured at 570 nm using a Spectra MAX M5 microplate spectrophotometer (Molecular Devices, Sunnyvale, CA, USA) after shaking for 15 s on a shaker. The data presented are representative of three independent experiments.

Immunofluorescence analysis

The cells were inoculated into a 24-well plate covered with glass coverslips (14 mm × 14 mm) at a density of 20,000 cells/well. After 48 h of cell growth, the cells were starved for 6 h in serum-free medium, the medium was replaced with complete medium, and the cells were stimulated with 5 ng/mL TGF-β1. After 1 h, NIF (10 μM) was added, and treatment was started 24 h later. The cells were fixed with 4% paraformaldehyde for 15 min at room temperature, washed with PBS 3 times for 5 min each, permeabilized with 0.5% Triton X-100 for 20 min, washed with PBS 3 times for 5 min each and blocked with 5% BSA and 0.05% Triton X-100 for 30 min. After blocking, the cell samples were incubated with anti-E-cadherin (1:500; Abcam, Cambridge, MA, USA) and α-SMA (1:200; Abcam, Cambridge, MA, USA) primary antibodies overnight at 4°C, followed by Cy3-labelled goat anti-mouse immunoglobulin G (IgG; Beyotime, Shanghai, China) at a 1:200 dilution (red) or FITC-488-labelled goat anti-mouse immunoglobulin G (IgG; Beyotime, Shanghai, China) at a 1:200 dilution (green). The cell nuclei were

counterstained with 4', 6-diamidino-2-phenylindole (Biosharp, Hefei, China). Immunofluorescence was analysed under a fluorescence microscope (Nikon 80i, Tokyo, Japan).

Wound migration assay

Cells were seeded into 6-well plates at a density of 10^5 cells/well. When the cells reached 80% confluence, they were starved for 6 h in serum-free medium, scratched with 0.01 mL pipette tips, and washed twice with normal saline. Then, the medium was replaced with complete medium, and the cells were stimulated with 5 ng/mL TGF-β1. After 1 h, NIF (10 μM) was added, and after 24 h of incubation, the cells were photographed with a microscope (Olympus, IX73, Japan). The cell migration rate was calculated as the ratio of the area of the migrated cells to the original scratched area.

Cell/lung lysate and Western blot

Protein experiments were performed according to previous reports[19]. Cells were inoculated into a Petri dish (10 cm) and then treated with the same immunofluorescence procedure as those collected after 24 h of NIF administration. The tissue was frozen in liquid nitrogen and ground to a powder in a mortar. Cell and tissue samples were lysed in RIPA (Beyotime, Shanghai, China) and centrifuged to collect the protein in the supernatant. The protein concentration of each sample was quantified via the Bradford method before loading. Then, the proteins were separated on 7.5–10% SDS-PAGE gels (Chengdu Baihe Technology Co., Ltd.) and transferred onto a 0.45 μM PVDF membrane (Merck Millipore, Billerica, MA, USA). After blocking in 5% (M/V) nonfat milk for 1 h, the membrane was incubated with antibodies overnight at 4°C. Then, the membrane was incubated with goat anti-rabbit or anti-mouse IgG (ZSGB-BIO Co., Beijing, China) at a 1:3,000 dilution for 60 min at 37°C. The reactive bands were identified using an enhanced chemiluminescence kit (Merck Millipore, Billerica, MA, USA). Then, the images were analysed using Image J computer software (National Institute of Health, Bethesda, MD, USA).

Thermal Drift Assay

According to the methods reported in the literature, some modifications were made[20]. The cells were cultured according to the method of protein extraction as we have described. After treated with NIF 200 μm for 2 hours, the cells were collected and the proteins in the cells were extracted. Divide the obtained protein evenly into 10 equal parts, and heat them at 45, 50, 55, 60, 65, 70, 75, 80, 85, 90°C for 6 min respectively, then centrifuge again at 4°C, 13300 r/15 min and The final protein is obtained by removing the supernatant. Then the protein image was finally obtained according to the method described.

Isolation and culture of lung fibroblasts

Wistar rats (180–220 g) were purchased from Vital River (Beijing, China). Wistar rats were anaesthetized with 10% chloral hydrate and then intratracheally administered BLM (5 mg/kg). After 7 days, blood was collected from abdominal aorta and rats were sacrificed. An intact lung tissue was obtained by dissection. Then, the lungs of the rats were washed with Hanks solution and chopped and digested with trypsin. After incubation at 37°C for 40 min followed by centrifuged at 1500 rpm for 5 min, the precipitate

was collected, medium was added, and the precipitate was mixed at 800 rpm for 5 min. The supernatant was centrifuged at 1500 rpm for 5 min, and the precipitate, which contained lung fibroblasts, was collected. The extracted primary lung fibroblasts were cultured in DMEM/F-12 (Gibco, NY, USA) medium containing 10% FBS and 1% penicillin and streptomycin in 5% CO_2 at 37°C. The cells were used between passages 3 and 8.

Animal studies of fibrosis

C57BL/6 mice (6–10 weeks old) were purchased from Huafukang (Beijing, China). C57BL/6 mice were anaesthetized with 10% chloral hydrate and then intratracheally administered BLM (2 mg/kg in the preventive group and 1 mg/kg in the therapeutic group); the sham-operated group was instilled with physiological saline. The mice were divided into 4 groups. The sham-operated group was intraperitoneally injected with physiological saline every day. The solvent group was intraperitoneally injected with normal saline. The NIF groups received low-dose NIF (25 mg/kg) or high-dose NIF (50 mg/kg).

H&E and Masson's trichrome staining

The lungs of the mice were immersed in 4% paraformaldehyde for a week and then processed for paraffin embedding. The paraffin-embedded pulmonary specimens were sectioned into 4-mm-thick slices, deparaffinized in xylene for 15 min, hydrated in gradient alcohol solutions, and then rinsed with 1% phosphate-buffered saline three times. Thereafter, these slices were stained with haematoxylin and eosin and Masson's trichrome for morphologic detection according to the manufacturers' standard protocols. Fibrosis was scored as described previously[21]. Fibre volume fractions were determined using Image J.

Hydroxyproline assay

The lung tissues were weighed, homogenized and subsequently hydrolysed by alkaline hydrolysis. The hydroxyproline levels were determined by a hydroxyproline detection kit according to the manufacturer's instructions (Nanjing Jiancheng Bioengineering Institute, Nanjing, China).

Immunohistochemical staining

Immunohistochemical (IHC) staining of the lungs was performed as described previously[22]. Paraffin-embedded lung sections were stained with primary antibodies (α-SMA, Collagen I and p-Stat3 (TY705)) using the DAB Detection Kit (ZSGB-BIO Co., Beijing, China).

Number of immune cells in lung tissue

Lung tissue was disrupted according to a previously described method and lysed with collagenase (37°C for 90 min)[22]. Changes in the cell ratio were detected by flow cytometry (BD LSR II) after incubation with different antibodies. The data were analysed by FlowJo software.

ELISA

The levels of TNF-α, IL-17A, IL-2 and others in the murine serum and BALF were analyzed by ELISA using commercially available kits (Cell Signaling Technology Company, MA, USA) according to the manufacturer's instructions.

Statistical analysis

The data are represented as the mean ± SD of three independent experiments. Two-tailed Student's t-test and One-way ANOVA were used for statistical analysis, and statistically significant P-values were as follows: *P < 0.05, **P < 0.01, ***P < 0.001; ****P < 0.0001; $^{\#}$P < 0.05, $^{\#\#}$P < 0.01, $^{\#\#\#}$P < 0.001, $^{\#\#\#\#}$P < 0.0001. Statistical analysis was performed using GraphPad Prism 6.0 (GraphPad software, San Diego, CA, USA).

Results

NIF could combine with Stat3

Although NIF has previously been reported to be a potential inhibitor of Stat3[15], we verified this using molecular docking. As shown in Fig. 1a, b, NIF is capable of forming intermolecular hydrogen bonds with GLU638, MET660 of the SH2 domain, making the complex stable; Moreover, the benzene ring moiety forms a conjugation with TYR657, ILE659. Together, these interactions promote the binding of NIF to Stat3. The docking results showed that the interaction energy score of the NIF and Stat3 was 22.4538, indicating that NIF could stably bind to Stat3. In addition, as shown in Fig. 1c, d, Stat3 gradually degrades with increasing temperature, but compared with the control group, NIF reduces its degradation level at high temperature in A549 and NIH/3T3 cell lines. It was further confirmed that NIF could bind to Stat3, indicating that it is a potential inhibitor of Stat3.

NIF reduces inflammatory responses in BLM-induced pulmonary fibrosis in vivo

First, we evaluated the effect of NIF on BLM-induced pulmonary fibrosis in mice. According to our previous research on NIF [14, 22], intraperitoneal administration (25 mg/kg or 50 mg/kg) was selected for *in vivo* experiment. As shown in Fig. 2a, we administered NIF to mice beginning on the first day of bronchial instillation of BLM (2-2.5 mg/kg) for a total of 28 days. After 28 days, BLM induced severe pulmonary fibrosis in mice, which resulted in a significant increase in the lung weight coefficient. Compared with the vehicle, NIF reduced the lung weight coefficient (Fig. 2b).

Furthermore, NIF reduced the BLM-induced increase in hydroxyproline levels (Fig. 2c). Simultaneously, we measured levels of the pro-inflammation cytokines IL-6, IL-4, IL-1β, TNF-α and TGF-β1 and found that their expression in BALF was altered in a dose-dependent manner upon NIF treatment (Fig. 2d-g). In addition, the BLM-induced elevation of IL-4 and TNF-α were alleviated by NIF treatment in serum (Fig. 2h, i).

NIF inhibits pulmonary fibrosis induced by BLM

H&E and Masson staining showed that NIF alleviated BLM-induced structural damage in the lung and collagen proliferation, and the decrease in the fibrosis score and Collagen volume fraction (CVF%) also indicated that NIF reduced collagen proliferation and improved pulmonary interstitial fibrosis (Fig. 3a-c). α-SMA and Collagen I are important proteins for characterizing fibrosis. As shown in Fig. 3d, e, BLM induced pulmonary fibrosis in mice, resulting in an increase in the expression of α-SMA and Collagen I, while NIF inhibited the increase in the expression of α-SMA and Collagen I. Moreover, NIF also inhibited EMT transformation *in vivo*. As shown in Fig. 3e, NIF inhibited the decrease in E-cadherin expression. This suggests that NIF could inhibit BLM-induced pulmonary fibrosis and EMT *in vivo*. At the same time, we found that BLM induced the abnormal activation of Stat3 (Fig. 3d, e), while this abnormal activation was decreased by NIF, indicating that NIF may inhibit pulmonary fibrosis by blocking the abnormal activation of Stat3.

NIF regulates the immune microenvironment of the lung

In the early stage of fibrosis, the innate immune system in the body is mainly antagonistic to stimulation, while immune cells in damaged tissues also contribute to chronic inflammation and tissue remodelling by secreting growth factors, cytokines, and chemokines and activating the synthesis of the extracellular matrix[23, 24]. Therefore, strategies against immunosuppressive cells and cytokines may be very beneficial in the context of tissue fibrosis during chronic inflammation. We found that BLM induced an increase in the expression of immune cells, inducing of Gr-1$^+$ CD11b$^+$ (MDSCs), F4/80$^+$ CD11b$^+$ (macrophage), and CD4$^+$, CD4$^+$ CD69$^+$T lymphocyte cells. NIF reduced the number of these immune cells to closer to normal levels (Fig. 4a-d).

NIF reverses pulmonary fibrosis induced by BLM

To further determine the therapeutic effect of NIF on pulmonary fibrosis, we also examined the effects of delayed NIF treatment (25 mg/kg or 50 mg/kg), that is, NIF treatment beginning 14 days after injury induced by BLM (1 mg/kg) for a total of 14 days (Fig. 5a). The results showed that NIF prolonged the survival rate of mice (Fig. 5b), and reduced the content of hydroxyproline (Fig. 5c). It should be noted that the levels of IL-2, IL-4 and other factors in the mouse serum were further reduced by NIF (Fig. 5d-h). Notably, H&E and Masson staining results show that NIF stimulation reversed BLM-induced lung inflammation and collagen expression, as shown in Fig. 6a. The fibrosis score and CVF% were further confirmed (Fig. 6b, c). Additionally, the results of immunohistochemistry and protein analysis showed that NIF also inhibited the expression of α-SMA and Collagen I and inhibited EMT (Fig. 6d, e). This suggests that NIF promotes fibrosis resolution even when exposure to it is delayed.

NIF inhibits the activation of fibroblasts

Based on these findings, we further explored the potential mechanism of NIF and studied the effect of NIF on the activation of fibroblasts induced by TGF-β1. First, the MTT results showed that NIF inhibited the proliferation of pulmonary fibroblasts in a time- and concentration-dependent manner (Fig. 7a, b). Next, to determine the effect of NIF on the activation of fibroblasts induced by TGF-β1, we starved fibroblasts for

6 h, stimulated them with TGF-β1, and analysed the increase in fibrosis phenotype at the protein level by immunofluorescence and western blot. As shown in Fig. 7d-g, α-SMA and Collagen I were enhanced by stimulation with TGF-β1. These results are consistent with previous reports[25]. To exclude the inhibitory effect of drugs on the activation of fibroblasts stimulated by TGF-β1 due to cytotoxicity, we selected 20 μM, proliferation inhibition rate less than 50%, as the concentration of the drugs. Upon treatment with NIF, the fibrosis phenotype of fibroblasts was not significantly affected, but the increase in α-SMA and Collagen I induced by TGF-β1 was reduced (Fig. 7d-g). These results suggest that NIF significantly suppresses the activation of fibroblasts induced by TGF-β1. To further examine the anti-fibrotic effects of NIF in activated lung fibroblasts, we isolated lung fibroblasts from rats treated with BLM and performed several parallel studies[26]. The results showed that NIF inhibited the proliferation of activated lung fibroblasts in a concentration-dependent manner, as shown in Fig. 7c. The expression of α-SMA and Collagen I also decreased in a concentration-dependent manner after treatment with NIF (Fig. 7h). The results show that NIF could inhibit the activation of fibroblasts *in vitro*.

At the same time, we found that NIF inhibited the expression of p-Stat3 in the presence or absence of TGF-β1(Fig. 7f, g). In addition, in primary activated lung fibroblasts, NIF also decreased p-Stat3 in a concentration-dependent manner (Fig. 7h). This suggests that NIF suppresses the activation of Stat3. This is also consistent with the previous *in vivo* results.

NIF suppresses the EMT and migration of A549 cells

When local fibroblasts are inadequate for tissue repair and remodelling, pulmonary epithelial cells that undergo EMT are a sources of myofibroblast cells in pulmonary fibrosis, and the EMT and migration of pulmonary epithelial cells induced by TGF-β1 can promote the occurrence and development of pulmonary fibrosis *in vitro*[27–29]. Therefore, we used TGF-β1 to stimulate A549 cells, which caused A549 cells to undergo metastasis and EMT. The MTT toxicity test was used to detect the inhibitory effect of NIF on the proliferation of A549 lung epithelial cells. NIF inhibited the proliferation of A549 cells in a time- and concentration-dependent manner (Fig. 8a). According to the MTT results, we chose a concentration of 20 μM and then induced the EMT and migration of A549 cells after 24 h of exposure to TGF-β1. As shown in Fig. 8b, c, the induction of A549 cell migration by TGF-β1 was increased compared with that the control group, but the induction of migration by TGF-β1 was inhibited after NIF was given. The results show that NIF could inhibit the migration of epithelial cells.

Regarding EMT, it can be seen from Fig. 8d, e that TGF-β1 stimulation reduced the protein expression of the epithelial marker E-Cadherin in A549 cells and increased the expression of the interstitial markers Vimentin and α-SMA. NIF inhibited the decrease in E-cadherin induced by TGF-β1 and the increase in Vimentin and α-SMA. The results show that NIF may inhibit the induction of EMT in A549 cells induced by TGF-β1.

We also detected the activation of Stat3 in pulmonary epithelial cells, as in fibroblasts, and found that NIF inhibited the expression of Stat3 in A549 cells in the presence or absence of TGF-β1 (Fig. 8e). These

results suggest that the improvement in pulmonary fibrosis induced by NIF *in vitro* may be related to the inhibition of the abnormal activation of Stat3.

Discussion

The potential mechanism of specific pulmonary fibrosis is difficult to understand, but the role of myofibroblasts in the development of pulmonary fibrosis has been recognized. Myofibroblasts are the primary effector cells of pulmonary fibrosis. At present, the most important sources of myofibroblasts are the transformation of resident fibroblasts, the differentiation of circulating bone marrow derived progenitor cells and the EMT of epithelial derived cells[30]. Thus, we mimicked the activation of fibroblasts and the EMT of epithelial cells by TGF-β1 to mimic the source of myofibroblasts in vitro. When activated, fibroblasts exhibited phenotypes such as those characterized by the expression of α-SMA and collagen I (Fig. 7)[31]. In a model of BLM-induced pulmonary fibrosis in mice, the expression levels of α-SMA and Collagen I were also significantly increased (Figs. 3 and 6). NIF was shown to inhibit the production of α-SMA and Collagen I induced by TGF-β1 *in vitro* and inhibit the increase in BLM-induced α-SMA and Collagen I *in vivo*. This inhibitory effect on myofibroblasts was also confirmed in the toxicity test of BLM-induced primary myofibroblasts (Fig. 7c), and it was demonstrated that BLM-induced myofibroblasts may be differentiated bone marrow progenitor cells[32]. These results suggest that NIF suppresses the origin of some myofibroblasts and the deposition of ECM components by inhibiting the transformation of fibroblasts to myofibroblasts, thus achieving partial pulmonary fibrosis inhibition.

In pulmonary fibrosis, EMT is a process in which pulmonary epithelial cells undergo phenotypic transformation into mesenchymal cells, usually fibroblasts and myofibroblasts[33]. Pulmonary epithelial cells are critically involved in fibrosis formation through a series of processes from early epithelial damage to fibroblastic EMT[34]. Our data demonstrated that A549 epithelial cells were stimulated by TGF-β1 to undergo EMT transformation, as they possessed the characteristics of myofibroblasts, namely, spindle-shaped morphology and expression of various mesenchymal immune cytochemical markers, such as α-SMA and Collagen I (Fig. 8). These substances are key mediators of ECM, structural remodelling, and the destruction of alveolar capillary units during and after lung injury[35]. NIF inhibited these changes after A549 cells were stimulated with TGF-β1, thereby reducing the number of epithelial-derived myofibroblasts and the expression of some types of collagen, ECM proteins, and the like (Fig. 8). These results were also confirmed *in vivo* (Figs. 3 and 6). More importantly, there are data showing that the alveolar epithelium is the main source of TGF-β1 during lung injury and fibrosis and that TGF-β1 in turn regulates the function and differentiation of fibroblasts, which further aggravates the development of pulmonary fibrosis[36]. Therefore, inhibiting the EMT of epithelial cells can largely inhibit pulmonary fibrosis.

In pulmonary fibrosis, some immune cells besides myofibroblasts are also involved in the development of diseases, and congenital and adaptive immunity contribute to the fibrogenesis of many organs[37]. Among these immune cells, macrophages are key regulators of fibrosis that are usually found in the vicinity of collagen-producing myofibroblasts and can secrete many profibrotic soluble mediators,

chemokines and matrix metalloproteinases, including TGF-β1[38–40]. The depletion of macrophages may improve pulmonary fibrosis. MDSCs are highly expressed in IPF patients and are inversely related to lung function in IPF, indicating that controlling MDSC expansion and accumulation or blocking T cell suppression represents a promising treatment for IPF[41]. The location of T lymphocyte accumulation is the largest in the area of lung tissue with inter-tissue fibrosis and honeycomb changes, and there are only a few T cells in the area of relatively normal tissue[42]. $CD4^+$ T lymphocytes specialize in the production of soluble factors (cytokines), which may play a role through fibrosis (IL-4, IL-13, TGF-β, IL-17A) [43]. In addition, inflammatory factors also regulate the TGF-β1-mediated pathway, and pro-inflammatory cytokines IL-1β, TNF-α and IFN-γ enhance TGF-β1-induced EMT by up regulating TGF-β receptor type I[44]. The results of this study found that NIF regulates BLM-induced imbalance of macrophages, MDSCs and T lymphocytes in lung tissue. In addition, NIF also inhibits the expression of inflammatory factors in alveolar lavage fluid and serum. These results demonstrate that NIF can further improve BLM-induced pulmonary fibrosis through immunosuppressive effects.

Stat3 is a protein that is potentially widely expressed in cells. It is instantaneously activated by a large number of different ligands and plays an important role in the occurrence and development of specific pulmonary fibrosis. The inhibition of Stat3 can weaken the sensitivity of IPF patients to exogenous TGF-β1, further block the transformation of fibroblasts into myofibroblasts induced by TGF-β1 and the release of collagen from fibroblasts, and improve two types of mouse models of skin fibrosis[11, 45]. Our results also showed that stimulation with TGF-β1 in vitro induced stat3 activation and that BLM infusion in vivo induced a significant number of p-Stat3-positive cells. All of these findings suggest that the excessive activation of Stat3 exacerbates pulmonary fibrosis. Therefore, NIF as an inhibitor of Stat3, significantly inhibits the over-activation of Stat3 *in vitro* and *in vivo* without affecting Stat3 in cells under normal conditions. This is the most ideal case and indicates that NIF could inhibit the excessive activation of Stat3 signalling in pulmonary fibrosis and improve pulmonary fibrosis. In addition, the activation of Stat3 also promotes EMT in the lungs, and excessive Stat3 signalling allows the lungs to be sensitive to other environmental stimuli or cytokines produced by inflammatory events, including those induced by activated innate lymphoid cells (ILC) or macrophages[46, 47]. Therefore, our drug reduces the excessive activation of Stat3 in pulmonary fibrosis, thereby inhibiting a number of processes, such as EMT, and the expression of some inflammatory cells such as MDSCs and macrophages may achieve a certain effect of improving pulmonary fibrosis.

Conclusion

Overall, in this article, we demonstrate that NIF ameliorates and reverses pulmonary fibrosis, but a more detailed understanding of the mechanism is worth studying. There are still some shortcomings of the *in vivo* administration and dosage of NIF that need to be improved. There is currently no good treatment for pulmonary fibrosis, and our findings have provided some strategies for the treatment of pulmonary fibrosis.

Abbreviations

IPF: idiopathic pulmonary fibrosis; BLM: bleomycin; NIF: nifuroxazide; TGF-β1: transforming growth factor-β1; EMT: epithelial-mesenchymal transition; Stat3: signal transduction and activator of transcription 3; human pulmonary fibroblasts: HPF; rat primary lung fibroblasts: RPLF; IL-6: interleukin-6; IL-4: interleukin-4; IL-1β: interleukin-1β; IL-17A: interleukin-17A; IL-10: interleukin-10; TNF-α: tumor necrosis factor α; ELISA: enzyme-linked immunosorbent assay; MDSCs: myeloid-derived suppressor cells; DAPI: 4',6-diamidino-2-phenylindole; FBS: fetal bovine serum; H&E: hematoxylin and eosin; IHC: immunohistochemistry; PBS: phosphate-buffered saline; BALF: bronchoalveolar lavage fluid; FVC: forced vital capacity; α-SMA: alpha-smooth muscle actin; CVF: Collagen volume fraction.

Declarations

Funding

This work paper was supported by the grants from the National Natural Science Foundation of China (81500054) and the National S&T Major Special Project on Major New Drug Innovations (2019ZX09201001, 2018ZX09711001-011).

Acknowledgements

The authors gratefully thank the staff of (Cell Signaling Technology Company, MA, USA) for cytokine testing.

Author Contributions

Conceived and designed the experiments: TY, CG and ZT. Performed the experiments: CG, QZ, GW, HL, LW, YL, and ZT. Analyzed the data: CG, QZ, YL, and TY. Contributed reagents/materials/analysis tools: LY, YX, WY, YY, LO. Wrote the manuscript: CG, TY. All authors read and approved the final manuscript.

Ethics approval and consent to participate

All animal experiments were approved by the Institutional Animal Care and Treatment Committee of Sichuan University in China (New Permit Number: 20171205-3).

Consent for publication

Not applicable.

Competing interests

The authors confirm that they have no conflict of interest with the content of this article.

Availability of data and materials

We would like to share part of our data, because some of our data will be used in future research.

References

1. Martinez FJ, Collard HR, Pardo A, Raghu G, Richeldi L, Selman M, Swigris JJ, Taniguchi H, Wells AU: **Idiopathic pulmonary fibrosis.** *Nature Reviews Disease Primers* 2017, **3:**17074.

2. Brett L, Collard HR, King TE: **Clinical course and prediction of survival in idiopathic pulmonary fibrosis.** *Am J Respir Crit Care Med* 2011, **183:**431-440.

3. Thomson CC, Duggal A, Bice T, Lederer DJ, Wilson KC, Raghu G: **2018 Clinical Practice Guideline Summary for Clinicians: Diagnosis of Idiopathic Pulmonary Fibrosis.** *Annals of the American Thoracic Society* 2019, **16:**285-290.

4. Puglisi S, Torrisi SE, Giuliano R, Vindigni V, Vancheri C: **What We Know About the Pathogenesis of Idiopathic Pulmonary Fibrosis.** *Semin Respir Crit Care Med* 2016, **37:**358-367.

5. Khalil N, O'Connor R: **Idiopathic pulmonary fibrosis: current understanding of the pathogenesis and the status of treatment.** *CMAJ : Canadian Medical Association journal = journal de l'Association medicale canadienne* 2004, **171:**153-160.

6. Karimi-Shah BA, Chowdhury BA: **Forced Vital Capacity in Idiopathic Pulmonary Fibrosis — FDA Review of Pirfenidone and Nintedanib.** *New England Journal of Medicine* 2015, **372:**1189-1191.

7. Yoon H-Y, Park S, Kim DS, Song JW: **Efficacy and safety of nintedanib in advanced idiopathic pulmonary fibrosis.** *Respiratory Research* 2018, **19:**203.

8. Lancaster L, Albera C, Bradford WZ, Costabel U, du Bois RM, Fagan EA, Fishman RS, Glaspole I, Glassberg MK, King TE, et al: **Safety of pirfenidone in patients with idiopathic pulmonary fibrosis: integrated analysis of cumulative data from 5 clinical trials.** *BMJ Open Respiratory Research* 2016, **3:**e000105.

9. Ihn H: **Pathogenesis of fibrosis: role of TGF-β and CTGF.** *Current Opinion in Rheumatology* 2002, **14:**681.

10. Levy DE, Darnell JE: **STATs: transcriptional control and biological impact.** *Nature Reviews Molecular Cell Biology* 2002, **3:**651-662.

11. Pechkovsky DV, Prêle CM, Wong J, Hogaboam CM, McAnulty RJ, Laurent GJ, Zhang SSM, Selman M, Mutsaers SE, Knight DA: **STAT3-Mediated Signaling Dysregulates Lung Fibroblast-Myofibroblast Activation and Differentiation in UIP/IPF.** *The American Journal of Pathology* 2012, **180:**1398-1412.

12. Lim CP, Phan TT, Lim IJ, Cao X: **Stat3 contributes to keloid pathogenesis via promoting collagen production, cell proliferation and migration.** *Oncogene* 2006, **25:**5416-5425.

13. Pushpakom S, Iorio F, Eyers PA, Escott KJ, Hopper S, Wells A, Doig A, Guilliams T, Latimer J, McNamee C, et al: **Drug repurposing: progress, challenges and recommendations.** *Nature Reviews Drug Discovery* 2019, **18:**41-58.

14. Yang F, Hu M, Lei Q, Xia Y, Zhu Y, Song X, Li Y, Jie H, Liu C, Xiong Y, et al: **Nifuroxazide induces apoptosis and impairs pulmonary metastasis in breast cancer model.** *Cell Death & Disease* 2015, **6:**e1701.

15. Nelson EA, Walker SR, Kepich A, Gashin LB, Hideshima T, Ikeda H, Chauhan D, Anderson KC, Frank DA: **Nifuroxazide inhibits survival of multiple myeloma cells by directly inhibiting STAT3.** *Blood* 2008, **112:**5095.

16. Zhao T, Jia H, Cheng Q, Xiao Y, Li M, Ren W, Li C, Feng Y, Feng Z, Wang H, Zheng J: *Nifuroxazide prompts antitumor immune response of TCL-loaded DC in mice with orthotopically-implanted hepatocarcinoma.* 2017.

17. Elsherbiny NM, Zaitone SA, Mohammad HMF, El-Sherbiny M: **Renoprotective effect of nifuroxazide in diabetes-induced nephropathy: impact on NFκB, oxidative stress, and apoptosis.** *Toxicology Mechanisms and Methods* 2018, **28:**467-473.

18. Vanommeslaeghe K, Hatcher E, Acharya C, Kundu S, Zhong S, Shim J, Darian E, Guvench O, Lopes P, Vorobyov I, Mackerell Jr. AD: **CHARMM general force field: A force field for drug-like molecules compatible with the CHARMM all-atom additive biological force fields.** *Journal of Computational Chemistry* 2010, **31:**671-690.

19. Lin C-C, Mabe NW, Lin Y-T, Yang W-H, Tang X, Hong L, Sun T, Force J, Marks JR, Yao T-P, et al: **RIPK3 upregulation confers robust proliferation and collateral cystine-dependence on breast cancer recurrence.** *Cell Death & Differentiation* 2020.

20. Molina DM, Jafari R, Ignatushchenko M, Seki T, Larsson EA, Dan C, Sreekumar L, Cao Y, Nordlund P: **Monitoring Drug Target Engagement in Cells and Tissues Using the Cellular Thermal Shift Assay.** *Science* 2013, **341:**84-87.

21. Hübner R-H, Gitter W, Mokhtari NEE, Mathiak M, Both M, Bolte H, Freitag-Wolf S, Bewig B: **Standardized quantification of pulmonary fibrosis in histological samples.** *BioTechniques* 2008, **44:**507-517.

22. Ye TH, Yang FF, Zhu YX, Li YL, Lei Q, Song XJ, Xia Y, Xiong Y, Zhang LD, Wang NY: **Inhibition of Stat3 signaling pathway by nifuroxazide improves antitumor immunity and impairs colorectal carcinoma metastasis.** *Cell Death & Disease* 2017, **8:**e2534.

23. Meneghin A, Hogaboam CM: **Infectious disease, the innate immune response, and fibrosis.** *The Journal of Clinical Investigation* 2007, **117:**530-538.

24. Yang H-Z, Cui B, Liu H-Z, Chen Z-R, Yan H-M, Hua F, Hu Z-W: **Targeting TLR2 Attenuates Pulmonary Inflammation and Fibrosis by Reversion of Suppressive Immune Microenvironment.** *The Journal of Immunology* 2009, **182:**692-702.

25. Tatler AL, Gisli J: **TGF-β activation and lung fibrosis.** *Proceedings of the American Thoracic Society* 2012, **9:**130-136.

26. Wohlfahrt T, Rauber S, Uebe S, Luber M, Soare A, Ekici A, Weber S, Matei A-E, Chen C-W, Maier C, et al: **PU.1 controls fibroblast polarization and tissue fibrosis.** *Nature* 2019, **566:**344-349.

27. Kage H, Borok Z: **EMT and interstitial lung disease: a mysterious relationship.** *Current opinion in pulmonary medicine* 2012, **18:**517-523.

28. Willis BC, Borok Z: **TGF-β-induced EMT: mechanisms and implications for fibrotic lung disease.** *American Journal of Physiology-Lung Cellular and Molecular Physiology* 2007, **293:**L525-L534.

29. Yu H, Königshoff M, Jayachandran A, Handley D, Seeger W, Kaminski N, Eickelberg O: **Transgelin is a direct target of TGF-β/Smad3-dependent epithelial cell migration in lung fibrosis.** *The FASEB Journal* 2008, **22:**1778-1789.

30. McAnulty RJ: **Fibroblasts and myofibroblasts: Their source, function and role in disease.** *The International Journal of Biochemistry & Cell Biology* 2007, **39:**666-671.

31. Hinz B, Phan SH, Thannickal VJ, Galli A, Bochaton-Piallat M-L, Gabbiani G: **The Myofibroblast: One Function, Multiple Origins.** *The American Journal of Pathology* 2007, **170:**1807-1816.

32. Hashimoto N, Jin H, Liu T, Chensue SW, Phan SH: **Bone marrow–derived progenitor cells in pulmonary fibrosis.** *The Journal of Clinical Investigation* 2004, **113:**243-252.

33. Xu J, Lamouille S, Derynck R: **TGF-β-induced epithelial to mesenchymal transition.** *Cell Research* 2009, **19:**156.

34. Selman M, Pardo A: **Role of Epithelial Cells in Idiopathic Pulmonary Fibrosis.** *Proceedings of the American Thoracic Society* 2006, **3:**364-372.

35. Willis B, M duBois R, Borok Z: *Epithelial Origin of Myofibroblasts during Fibrosis in the Lung.* 2006.

36. Xu YD, Hua J, Mui A, O'Connor R, Grotendorst G, Khalil N: **Release of biologically active TGF-β1 by alveolar epithelial cells results in pulmonary fibrosis.** *American Journal of Physiology-Lung Cellular and Molecular Physiology* 2003, **285:**L527-L539.

37. Wynn TA: **Integrating mechanisms of pulmonary fibrosis.** *The Journal of experimental medicine* 2011, **208:**1339-1350.

38. Byrne AJ, Maher TM, Lloyd CM: **Pulmonary Macrophages: A New Therapeutic Pathway in Fibrosing Lung Disease?** *Trends in Molecular Medicine* 2016, **22:**303-316.

39. Murray LA, Chen Q, Kramer MS, Hesson DP, Argentieri RL, Peng X, Gulati M, Homer RJ, Russell T, van Rooijen N, et al: **TGF-beta driven lung fibrosis is macrophage dependent and blocked by Serum amyloid P.** *The International Journal of Biochemistry & Cell Biology* 2011, **43:**154-162.

40. Bonniaud P, Kolb M, Galt T, Robertson J, Robbins C, Stampfli M, Lavery C, Margetts P, B Roberts A, Gauldie J: *Smad3 Null Mice Develop Airspace Enlargement and Are Resistant to TGF- -Mediated Pulmonary Fibrosis.* 2004.

41. Fernandez IE, Greiffo FR, Frankenberger M, Bandres J, Heinzelmann K, Neurohr C, Hatz R, Hartl D, Behr J, Eickelberg O: **Peripheral blood myeloid-derived suppressor cells reflect disease status in idiopathic pulmonary fibrosis.** *European Respiratory Journal* 2016, **48:**1171-1183.

42. Parra ER, Kairalla RA, Ribeiro de Carvalho CR, Eher E, Capelozzi VL: **Inflammatory Cell Phenotyping of the Pulmonary Interstitium in Idiopathic Interstitial Pneumonia.** *Respiration* 2007, **74:**159-169.

43. Atamas SP, White B: **Cytokine regulation of pulmonary fibrosis in scleroderma.** *Cytokine & Growth Factor Reviews* 2003, **14:**537-550.

44. Liu X: **Inflammatory cytokines augments TGF-β1-induced epithelial-mesenchymal transition in A549 cells by up-regulating TβR-I.** *Cell Motility* 2008, **65:**935-944.

45. Chakraborty D, Šumová B, Mallano T, Chen C-W, Distler A, Bergmann C, Ludolph I, Horch RE, Gelse K, Ramming A, et al: **Activation of STAT3 integrates common profibrotic pathways to promote fibroblast activation and tissue fibrosis.** *Nature Communications* 2017, **8:**1130.

46. D. RC: **Innate Immune Cytokines, Fibroblast Phenotypes, and Regulation of Extracellular Matrix in Lung.** *Journal of Interferon & Cytokine Research* 2017, **37:**52-61.

47. Huang Q, Han J, Fan J, Duan L, Guo M, Lv Z, Hu G, Chen L, Wu F, Tao X, et al: **IL-17 induces EMT via Stat3 in lung adenocarcinoma.** *American journal of cancer research* 2016, **6:**440-451.

Figures

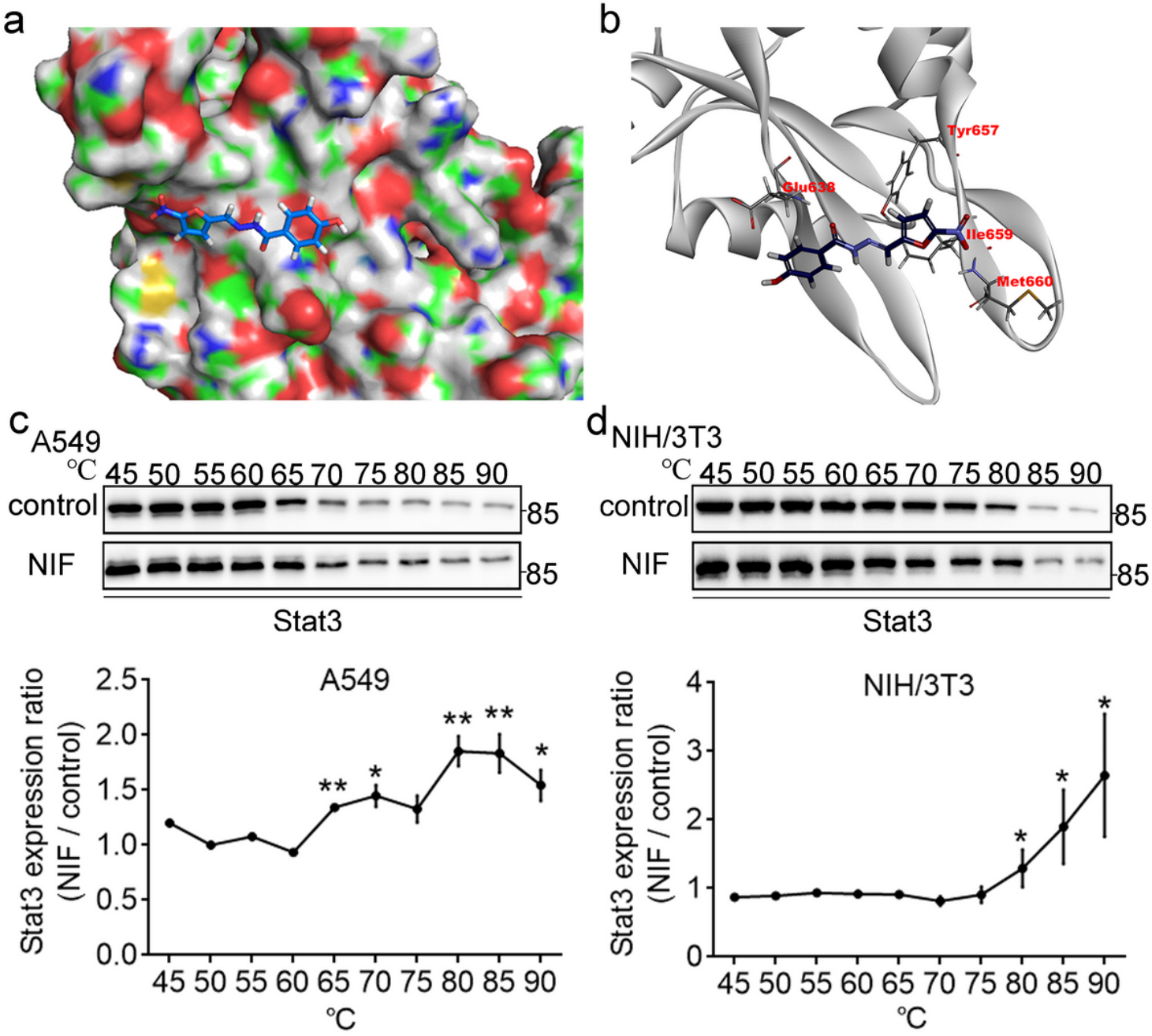

Figure 1

NIF could be combined with Stat3. (a) Surface of the electrostatic map. (b) Residues of Stat3. (c, d) Representative Western blots for the effects of NIF(200 μM) on thermal stabilization of Stat3 protein in A549 and NIH/3T3 cells. The relative expressions were quantified with Image J. Statistical significance was tested using Two-tailed Student's t-test; All data are expressed as mean ± SD, n = 3 *P < 0.05, **P < 0.01.

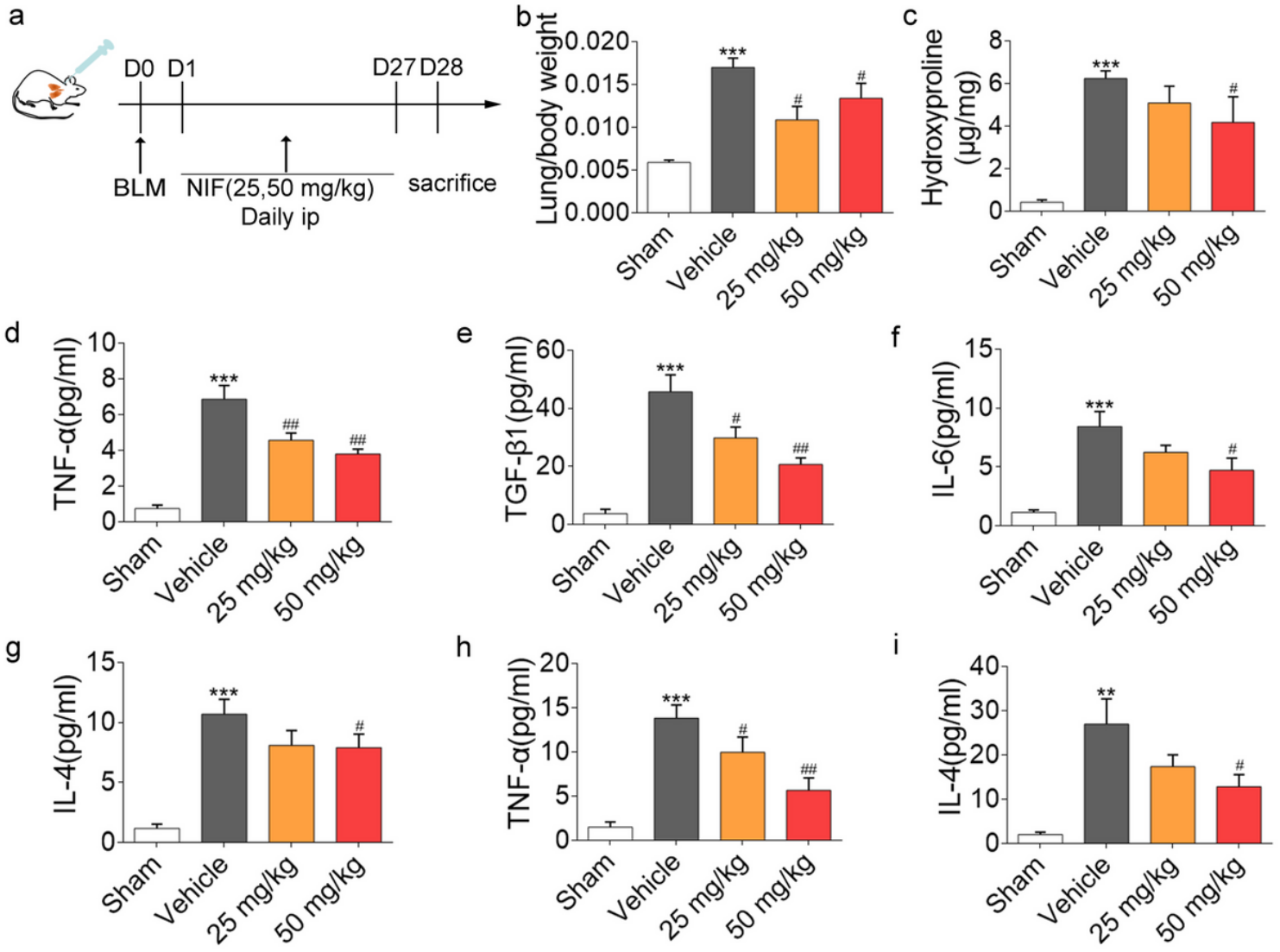

Figure 2

NIF reduces inflammation and expression of fibrotic markers in BLM-induced lung fibrosis. (a) Outline of the design of therapeutic dosing of NIF in mice with established fibrosis following BLM-induced lung injury. n = 5(Sham); n = 7 (Vehicle); n = 5 (NIF 25 mg/kg); n = 7 (NIF 50 mg/kg). (b) Lung weight coefficient of mice depicted in (a). (c) Quantitative analysis of hydroxyproline in lung homogenates from the groups of mice depicted in (a). (d-g) Analysis of TNF-α, IL-4, IL-6, and TGF-β1 levels in BALF of control and BLM-treated mice in the presence of vehicle, NIF. (h, i) Analysis of IL-4 and TNF-α levels in serum of control and BLM treated mice in the presence of vehicle, NIF. Statistical significance was tested using one-way ANOVA; All data are expressed as mean ± SD, n = 3 *P < 0.05, **P < 0.01, ***P < 0.001, ****P < 0.0001 vs sham; #P < 0.05, ##P < 0.01, ###P < 0.001, ####P < 0.0001 vs vehicle.

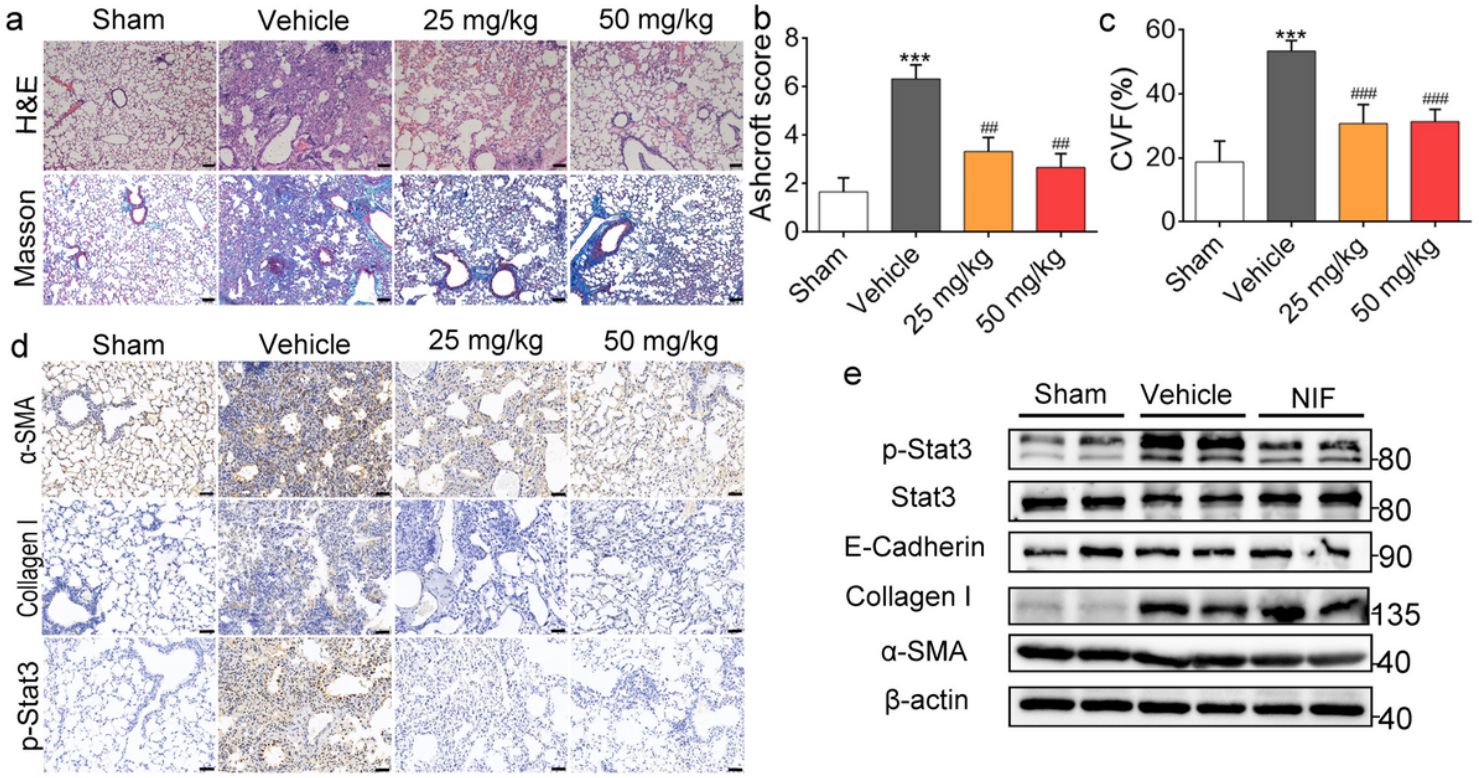

Figure 3

NIF inhibits pulmonary fibrosis induced by BLM. (a) Representative images show haematoxylin and eosin (H&E), Masson's trichrome. Scale bars, 100 μm. (b) Quantification of fibrosis on lung sections based on the results of H&E staining. (c) Quantification of collagen content volume fraction of lung sections based on Masson staining results. (d) Representative images show α-SMA, Collagen I, p-Stat3 staining of lung sections from the indicated groups of mice. Scale bars, 50 μm. (e) Representative immunoblots of p-Stat3, Stat3, α-SMA, Collagen I, E-Cadherin, and β-actin in lung homogenates of mice as indicated. NIF (50 mg/kg).Statistical significance was tested using one-way ANOVA; All data are expressed as mean ± SD, n = 3 - 5. ****P < 0.0001 vs sham; ###P < 0.001, ####P < 0.0001 vs vehicle.

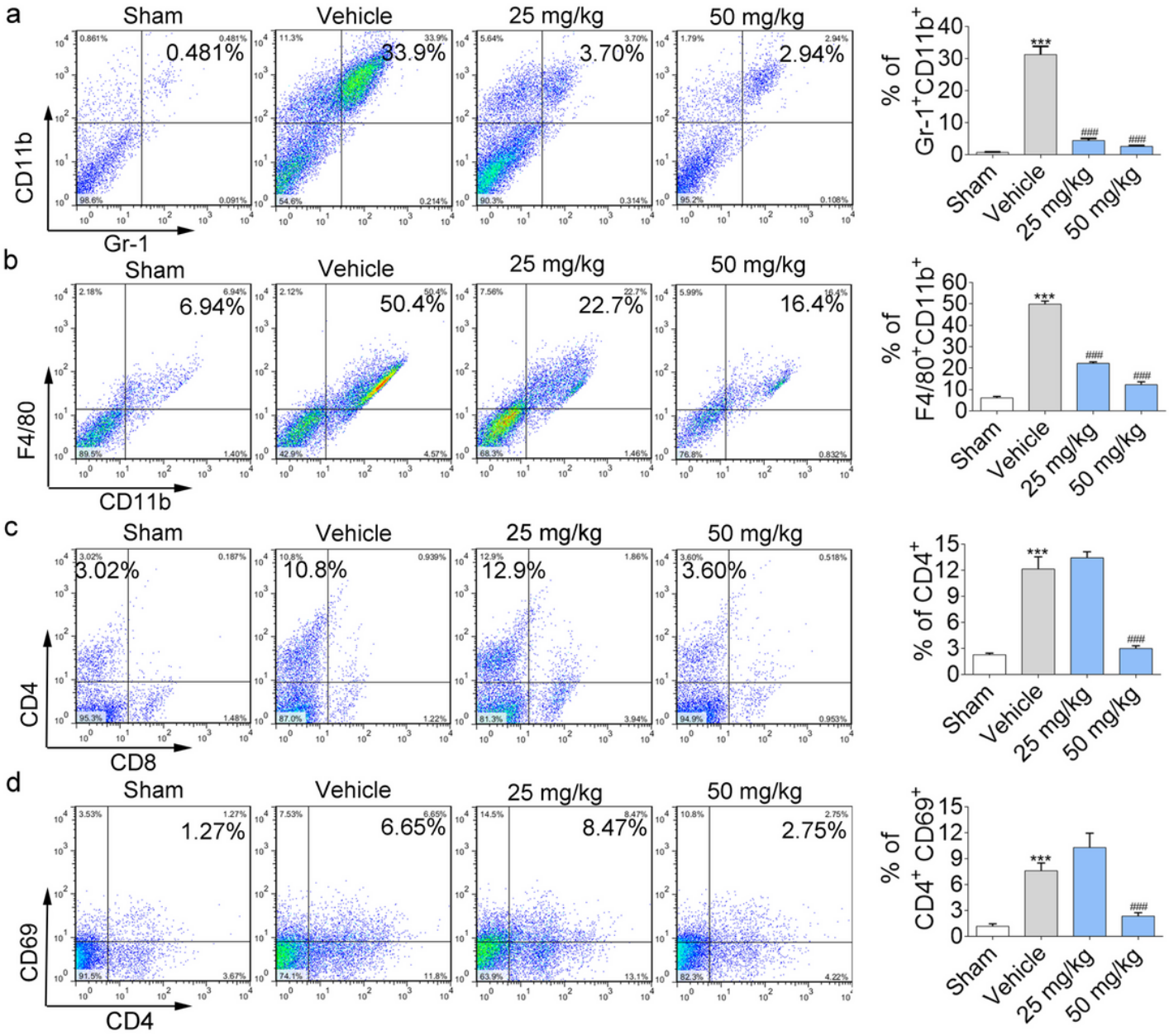

Figure 4

NIF regulates the immune microenvironment of the lungs. (a-d) Quantification of MDSCs, macrophage, and CD4+, CD4+CD69+T lymphocyte cells infiltration in the lung tissue of control and BLM-treated mice in the presence of vehicle, NIF. Statistical significance was tested using one-way ANOVA; All data are expressed as mean ± SD. ***P < 0.001, ****P < 0.0001 vs sham; ###P < 0.001, ####P < 0.0001 vs vehicle; n = 3.

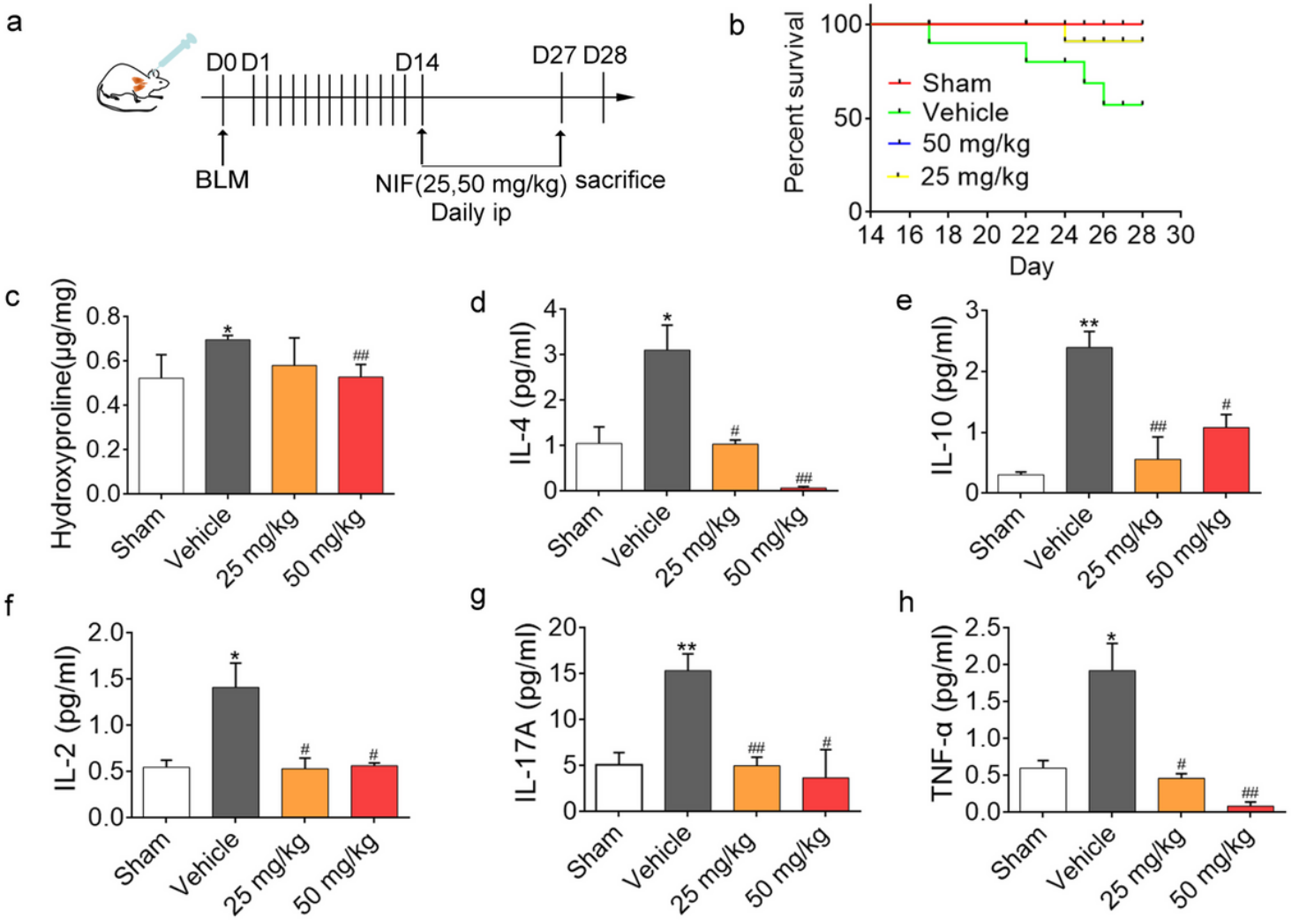

Figure 5

NIF promotes resolution of inflammation and improves survival in BLM induced lung fibrosis. (a) Outline of the design of therapeutic dosing of NIF in mice with established fibrosis following BLM-induced lung fibrosis. (b) Survival curves of mice. n = 4(Sham), n = 9(Vehicle), n = 8(25 mg/kg, 50 mg/kg). (c) Quantitative analysis of hydroxyproline in lung homogenates from the groups of mice depicted in A. Statistical significance was tested using Student's t-test. (d-h) Analysis of IL-2, IL-4, IL-10, L-17A, and TNF-α levels in serum of control and BLM treated mice in the presence of vehicle, NIF. Statistical significance was tested using one-way ANOVA. All data are expressed as mean ± SD, n = 3, *P < 0.05, **P < 0.01, ***P < 0.001 vs sham; #P < 0.05, ##P < 0.01, ###P < 0.001 vs vehicle.

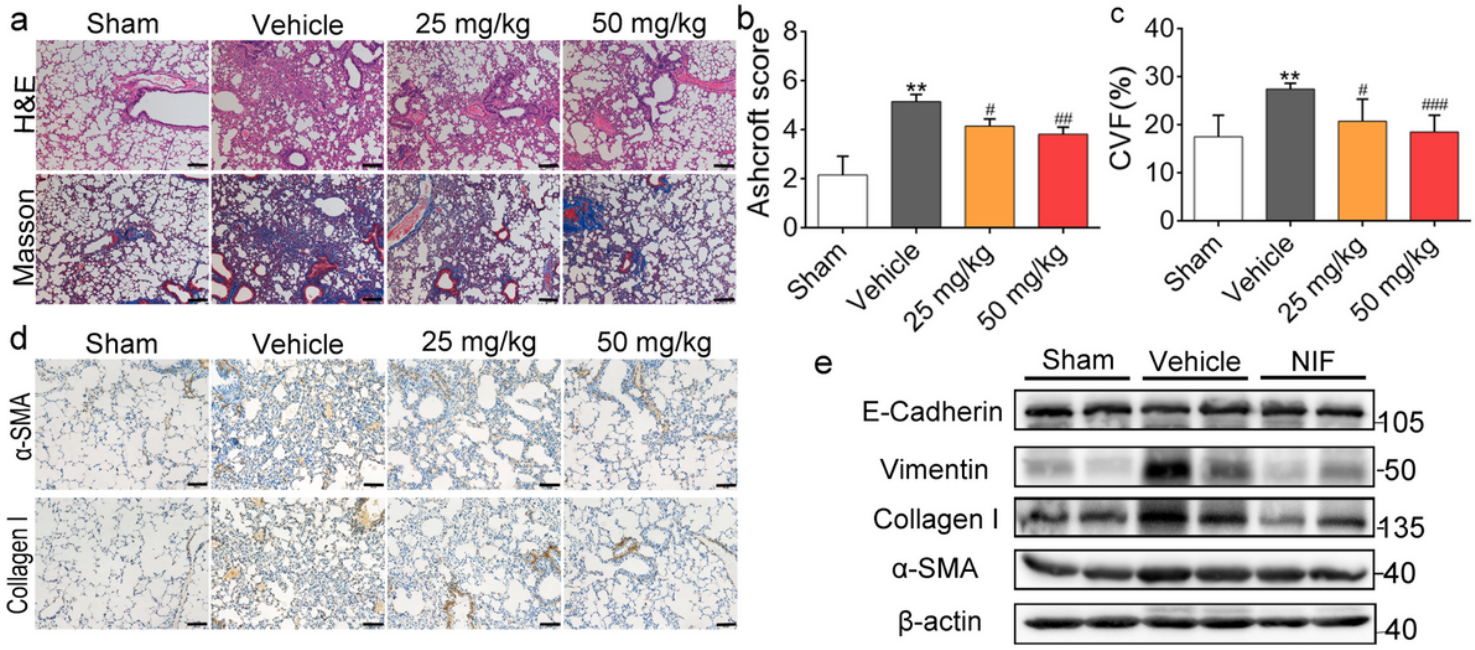

Figure 6

NIF reverses pulmonary fibrosis induced by BLM. (a) Representative images show haematoxylin and eosin (H&E), Masson's trichrome. Scale bars, 100 μm. (b) Quantification of fibrosis on lung sections based on the results of H&E staining. (c) Quantification of collagen content volume fraction of lung sections based on Masson staining results. (d) Representative images show α-SMA and Collagen I staining of lung sections from the indicated groups of mice. Scale bars, 50 μm. (e) Representative immunoblots of α-SMA, Collagen I, E-Cadherin, Vimentin, and β-actin in lung homogenates of mice as indicated. NIF (50 mg/kg). Statistical significance was tested using one-way ANOVA; All data are expressed as mean ± SD. n = 3 - 5. **P < 0.01, ***P < 0.001 vs sham; #P < 0.05, ##P < 0.01 vs vehicle.

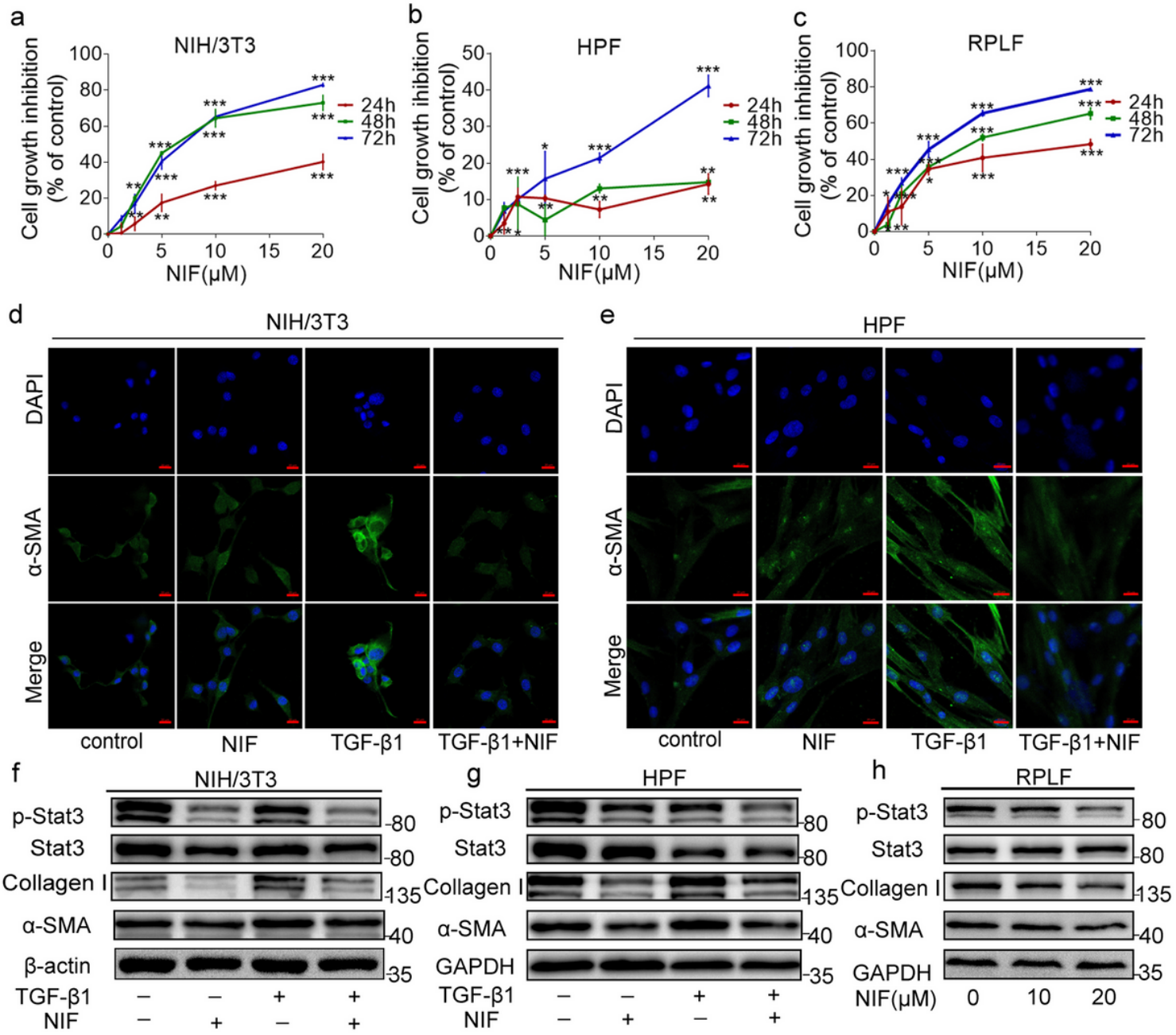

Figure 7

NIF inhibits the activation of fibroblasts. (a-c) NIH/3T3, HPF, and Rat primary lung fibroblasts (RPLF) were treated with different concentrations of NIF for 24, 48 or 72 h and cell viability was measured by the MTT assay. Statistical significance was tested using Student's t-test; each point represents the mean ± SD for at least 3 independent experiments (*P < 0.05; **P < 0.01; ***P < 0.001, ****P < 0.0001 vs vehicle control). (d, e)Representative fluorescent staining images of α-SMA (green) and nuclei (blue) in NIH/3T3 and HPF treated with TGF-β1 or NIF for 24 h. Scale bars, 20 μm. (f, g) Representative immunoblots of α-SMA Collagen I p-Stat3, Stat3, β-actin, and GAPDH from fibroblasts treated with TGF-β1 or NIF for 24 h. H Representative immunoblots of α-SMA Collagen I p-Stat3, Stat3, and GAPDH from RPLF stimulated with NIF (24 h).

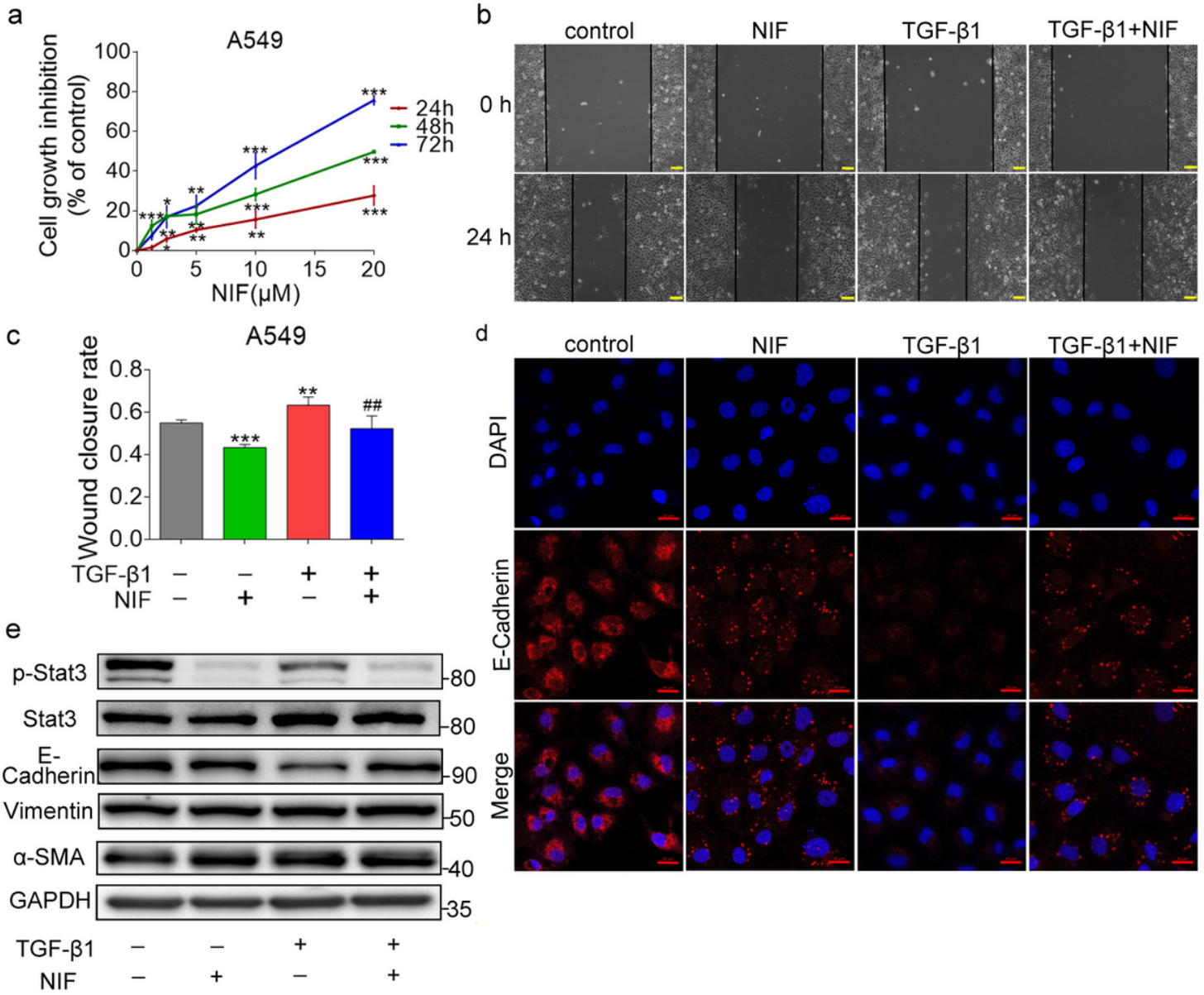

Figure 8

NIF suppresses EMT and migration of A549 induced by TGF-β1. (a) A549 were treated with different concentrations of NIF for 24, 48 or 72 h and cell viability was measured by the MTT assay. Statistical significance was tested using Student's t-test; each point represents the mean ± SD for at least 3 independent experiments. *P < 0.05; **P < 0.01; ***P < 0.001, ****P < 0.0001 vs vehicle control. (b) Representative images of migration in A549 treated with TGF-β1 or NIF for 24 h. Scale bars, 100 μm. (c) Quantified wound healing area ratio. Data are expressed as mean ± SD. n = 3, **P < 0.01, ***P < 0.001 vs control; ##P < 0.01 vs TGF-β1. (d) Representative fluorescent staining images of E-Cadherin (red) and nuclei (blue) in A549 treated with TGF-β1 or NIF for 24 h. Scale bars, 20 μm. (e) Representative immunoblots of α-SMA、E-Cadherin, Vimentin, p-Stat3, Stat3, and GAPDH from A549 treated with TGF-β1 or NIF for 24 h.

Supplementary Files

This is a list of supplementary files associated with this preprint. Click to download.

- Abstractfigure.png